J Mater Sci (2008) 43:4264–4270
DOI 10.1007/s10853-008-2618-x

Synthesis and properties of barium titanate stannate thin films by chemical solution deposition

Jon F. Ihlefeld · William J. Borland · Jon-Paul Maria

Received: 18 March 2008 / Accepted: 25 March 2008 / Published online: 17 April 2008

Abstract Barium titanate stannate ($BaTi_{1-x}Sn_xO_3$, $0 \leq x \leq 0.25$) thin films were deposited directly on copper foil substrates via a chelate chemical solution process. The films were subsequently crystallized in a reducing atmosphere such that substrate oxidation was avoided and that the 2-valent state of tin could be stabilized. Despite the stabilization of the low-melting temperature SnO oxidation state at high temperatures, the final grain size was smaller with increased tin incorporation similar to other *B*-site substituted $BaTiO_3$ films. Temperature and field-dependent dielectric measurements revealed a reduction in dielectric constant and dielectric tuning with increasing tin concentration. The reduction in permittivity with reduced grain size is consistent with the well-known trends for ceramic barium titanate and in combination with a defect-dipole model involving Sn acceptors, can be used to explain the experimental trends. Phase transition frequency dependence was studied and for compositions containing up to 25 mole percent tin. No phase transition dispersion was observed and thus no strong evidence of relaxor-like character. The phase transition became increasingly diffuse with deviation from Curie–Weiss behavior, but the observed transition temperatures agreed well with bulk reference data.

J. F. Ihlefeld · J.-P. Maria
Department of Materials Science and Engineering, North Carolina State University, Raleigh, NC 27695, USA

W. J. Borland
DuPont Electronic Technologies, Research Triangle Park, NC 27709, USA

Present Address:
J. F. Ihlefeld (✉)
The Pennsylvania State University, University Park, PA 16802, USA
e-mail: jfi2@psu.edu

Introduction

Barium strontium titanate (BST) and barium titanate zirconate (BTZ) thin films have been widely investigated for applications in tunable electronics, [1–3] dynamic random access memory, [4, 5] and decoupling capacitors [6]. Barium titanate stannate (BTS) is a chemically similar perovskite solid solution of the ferroelectric barium titanate and the linear dielectric barium stannate. Additions of barium stannate to barium titanate are known to result in a phase transition pinching effect, where the cubic-tetragonal transition temperature decreases and the tetragonal-orthorhombic and orthorhombic-rhombohedral transition temperatures increase [7–9]. As a result, compositions containing approximately 10 mole percent and greater levels of $BaSnO_3$ transition directly from cubic to rhombohedral. The phase transition pinching effect has important implications from a technological perspective in allowing for a flattened temperature response that is desirable for many device applications. Additionally, a transition to a diffuse phase transition with second order character at a 10 mole percent level followed by relaxor behavior with clear departure from Curie–Weiss transition behavior and a frequency dispersive T_{max} at the 20 mole percent level are observed [10–12]. While a wealth of information exists on BTS in bulk form, [7–11, 13] it has garnered considerably less attention in the thin film community. Of the BTS films studied, all display peak permittivities limited to less than 650, [14–20] and diminished dielectric tunability. These two features likely

result from fine grain dimensions and limited processing temperatures [21]. Decreased grain dimensions may stem from two sources: (i) low-processing temperature and (ii) incorporation of tin into the precursor gel, which may alter nucleation behavior or otherwise limit diffusion and densification and coarsening.

Recent advancements in base-metal/complex oxide thin film processing have been afforded by a successful marriage of bulk ceramic controlled atmosphere firing schedules and thin film deposition techniques. This was first demonstrated for ferroelectric films by Dawley et al. in the chemical solution deposition (CSD) of BST on nickel tapes [22, 23]. Using similar techniques it was shown that device quality perovskites of the barium titanate family could be deposited and processed on copper foil substrates [6, 24, 25]. While successful for preparing high permittivity dielectrics in contact with base-metal substrates, the temperature response of permittivity for pure barium titanate may be too sharp for many capacitor applications. To tailor the temperature response, zirconium and hafnium substitutions for titanium are routinely used in the bulk, and have been explored in thin films to pinch the phase transitions and achieve X7R characteristics. While successful in shifting the permittivity peak to lower temperatures and increasing transition diffuseness for thin film embodiments, a permittivity decrease was observed as the substituent level increased [24, 25]. This permittivity decrease was attributed to a grain size reduction [24]. What is required is a solid solution combination that provides the necessary phase transition shift, while allowing for the solid-state diffusion that supports grain growth. We have recently shown that the addition of fluxing agents including boron [26] and barium borate [27] can enhance dielectric properties by enabling grain growth and improving film crystallinity. We propose that the use of tin oxide, specifically with Sn^{2+}, i.e., SnO during densification, may achieve the desired fluxing effect as well as shift the phase transition temperature, thereby simplifying the solution preparation procedures.

The current investigation presents a methodology for depositing BTS thin films onto base-metal copper substrates via CSD. In doing so, the structure-property relationships are discussed in the context of developing a dielectric/substrate embodiment offering large grain size and an engineered temperature-dependent dielectric response sufficient for use in embedded passive technologies.

Experimental procedure

Dielectric compositions of $Ba(Ti_xSn_{1-x})O_3$ with ($0 \leq x \leq 0.25$) were prepared using a CSD technique. Precursor solutions containing barium, titanium, and tin were prepared via a chelate chemistry [28, 29]. Tin *n*-butoxide and titanium isopropoxide were combined and reacted with 2,4 pentanedione and diethanolamine as a chelating agents in a 1:2 ratio. Barium acetate was separately dissolved in glacial acetic acid and the two precursors were combined in an equimolar ratio, where solution stoichiometry was controlled by the constituent masses. The resulting solution was 0.3 M as referenced to barium concentration. The solution was spin cast onto 18-μm thick copper foils at 3,000 RPM for 30 s. The films were subsequently placed on a hotplate at 250 °C for 7 min and 30 s for solvent evaporation and gel consolidation. This process was repeated five times, resulting in films with an as-fired thickness of approximately 625 nm.

Films were heated at 30 °C/min to 900 °C, held for 30 min for crystallization and subsequently cooled to 150 °C before removal from the furnace. To protect the copper substrate from oxidation during the high-temperature crystallization anneal and to stabilize the 2-valent state of tin, a sufficiently reducing atmosphere must be employed. Figure 1 shows the pO_2—temperature equilibrium phase diagram for each of the metal species, oxygen, and the metal oxides [30]. The atmosphere-temperature space available to reduce copper and oxidize barium, titanium, and tin while stabilizing the SnO phase is highlighted. To tailor the atmosphere to the required conditions an equilibrium reaction established by hydrogen,

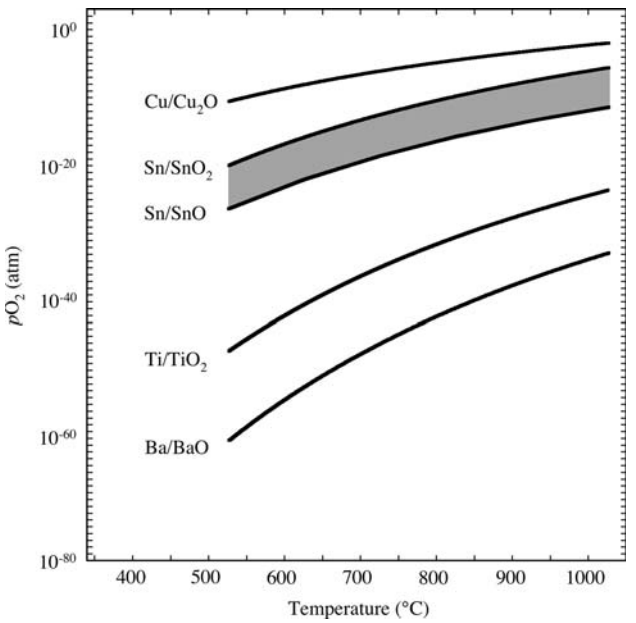

Fig. 1 Richardson-Ellingham diagram representing the equilibrium reactions of each of the metals, oxygen, and metal oxides in the barium titanate stannate on copper system. The shaded region represents the equilibrium pO_2-temperature conditions for SnO, BaO, TiO_2, metallic Cu, and O_2

oxygen impurities in carrier gases, and water vapor was achieved by flowing nitrogen from a liquid source and hydrogen containing forming gas through an H_2O bubbler at room temperature. Upon heating to 900 °C, this mixture results in an atmosphere containing a pO_2 of 10^{-13} atm with a total pressure of 1 atm, which is sufficient to oxidize all film species and protect the copper substrate in addition to stabilizing the Sn^{2+} state. The pO_2 was monitored in situ with a solid-state oxygen sensor (Australian Oxytrol Systems) to ensure proper conditions. A reoxidation anneal at 550 °C and 10^{-7} atm O_2 for 30 min was used to minimize electrically active point defects resulting from the low pO_2 and high-temperature crystallization anneal [31, 32]. We note that this reoxidation anneal should promote conversion of residual Sn^{2+} to Sn^{4+} and remove the potential for acceptor-like behavior of Sn on the B-site. 40 nm thick platinum top electrodes ($\sim 10^{-4}$ cm^2) were deposited through a shadow mask via DC magnetron sputtering to define metal-insulator-metal capacitor structures.

Phase assemblage in the film/foil stack was studied with a Bruker AXS D-5000 X-ray diffractometer equipped with a Hi-Star area detector. The film microstructures were characterized by atomic force microscopy (AFM) using a CP Research Thermomicroscopes Scanning Autoprobe in contact mode and by field-emission scanning electron microscopy (FE-SEM) with a JEOL 6400F instrument. Dielectric properties were studied as functions of electric field and temperature using a HP 4192 impedance analyzer and a modified MMR Technologies cryogenic temperature stage. Permittivity—field measurements were conducted at room temperature from −15 to 15 volts at 10 kHz with a 0.05 V oscillator. Phase transition behavior was studied by measuring the permittivity and loss tangent of the films from 100 K to 450 K at a 5 K/min ramp rate and zero DC bias with oscillator conditions ranging from 1 to 100 kHz and 0.05 V.

Results and discussion

$\theta-2\theta$ X-ray diffraction patterns for each composition are shown in Fig. 2. Diffraction peaks consistent with a perovskite phase and the copper substrate are identified in each composition. No additional peaks attributable to either tin oxide or copper oxide can be identified, suggesting that tin was fully incorporated into the lattice and that the reductive conditions were sufficient to protect the copper substrate. To verify that tin was incorporated into the lattice, lattice parameter measurements were conducted by collecting diffraction patterns of the *001*, *002*, and *003* peaks and calculating the lattice constant using a Nelson–Riley extrapolation [33] with the results shown in Fig. 3. The linear lattice parameter increase is consistent with the incorporation of the larger Sn ion on the perovskite *B*-site

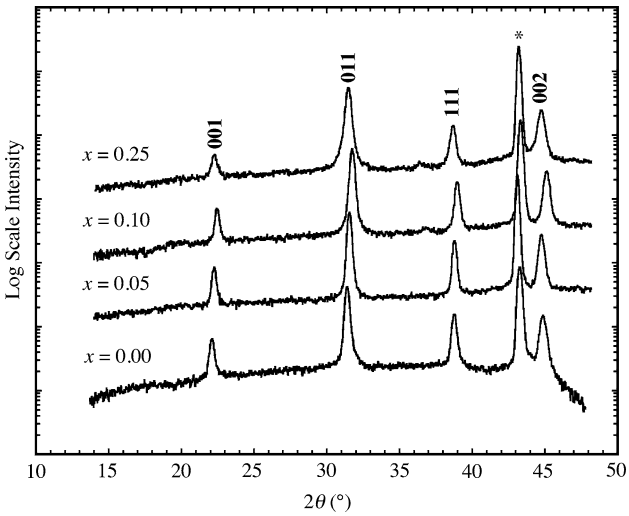

Fig. 2 $\theta-2\theta$ X-ray diffraction patterns of $BaTi_{1-x}Sn_xO_3$ ($0.0 \leq x \leq 0.25$) prepared and fired at 900 °C on copper substrates. * denotes substrate diffraction peak

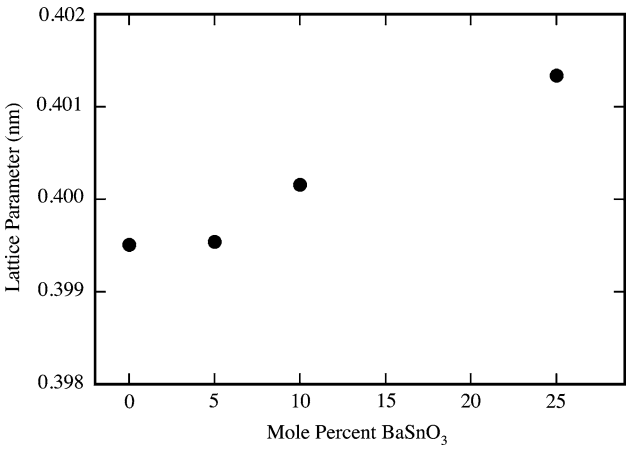

Fig. 3 Measured lattice parameters of $BaTi_{1-x}Sn_xO_3$ ($0.0 \leq x \leq 0.25$)

and indicates full barium stannate solubility for films containing up to 25% $BaSnO_3$.

Figure 4 shows 3 μm × 3 μm topographic AFM scans for each composition. A grain size decrease is observed, particularly for the composition containing 25% mole percent barium stannate. The average grain size was quantified using a linear intercept method with the results shown in Fig. 5 illustrating the grain size—composition relationship. The error bars indicate a 95% confidence interval in the measured grain diameters [34]. It should be noted that the decrease is not as pronounced as was observed in the BTZ [24] and barium titanate hafnate [25] compositions. This is particularly evident at the 25 mole percent level where the tin substituted samples had an average grain size of 95 nm and the zirconium and hafnium substituted films were 78 nm and 76 nm, respectively. This difference suggests that the SnO stabilization was

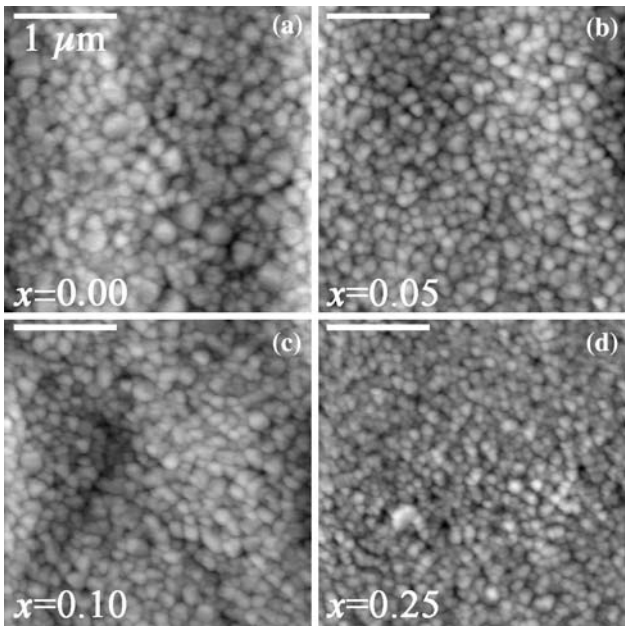

Fig. 4 3 μm × 3 μm topographic AFM scans for (**a**) $BaTiO_3$, (**b**) $BaTi_{0.95}Sn_{0.05}O_3$, (**c**) $BaTi_{0.90}Sn_{0.10}O_3$, and (**d**) $BaTi_{0.75}Sn_{0.25}O_3$

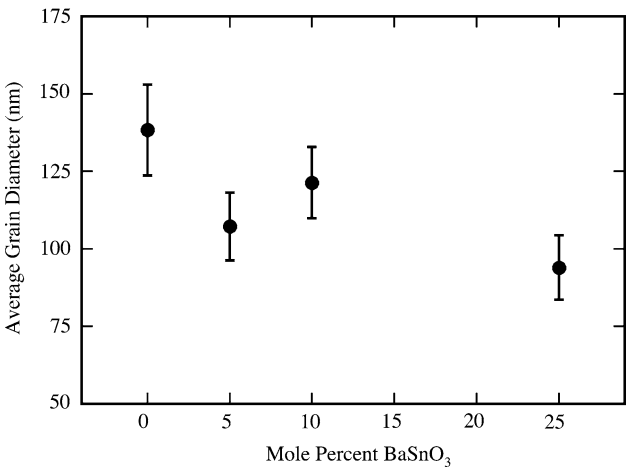

Fig. 5 Measured average grain size for $BaTi_{1-x}Sn_xO_3$ ($0.0 \leq x \leq 0.25$). Error bars indicate a 95% confidence interval for each measurement

successful in either limiting the grain size reduction by fluxing the system, or that the Sn did not change the nucleation and growth characteristics to the extent of Zr and Hf, which are suspected to inhibit grain growth via their refractory nature and to promote nucleation from the amorphous gel.

The temperature dependence of permittivity and loss tangent is shown in Fig. 6. Two distinct trends can be identified with increasing tin level: (i) the phase transition temperature, T_{max}, decreases and (ii) the maximum

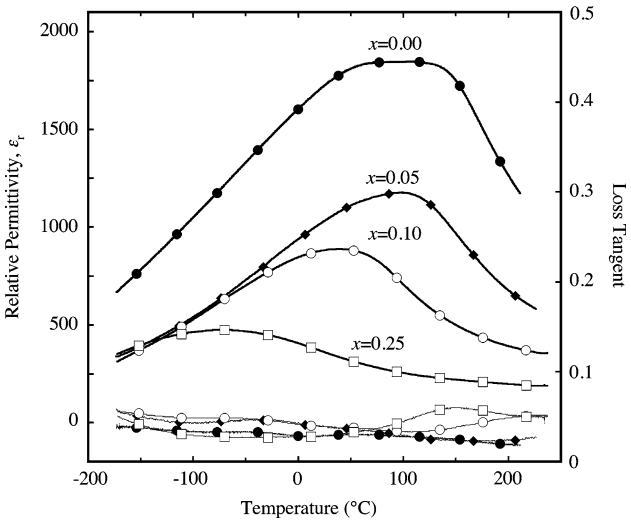

Fig. 6 Temperature dependence of permittivity and loss tangent for $BaTi_{1-x}Sn_xO_3$ ($0.0 \leq x \leq 0.25$) composition series

permittivity, ε_{max}, decreases. The phase transition temperature was plotted versus composition in Fig. 7 along with values from the bulk work of Smolenskii et al. [9]. The trend of transition temperature and composition is virtually identical in both the film and bulk systems further indicating complete solid solution formation. A permittivity decrease was expected given the grain size reduction, however the degree observed was more pronounced than in the $Ba(Ti,Zr)O_3$ and $Ba(Ti,Hf)O_3$ systems as shown in the maximum permittivity versus average grain diameter plot in Fig. 8, compared with a pure $BaTiO_3$ series [21]. For compositions containing 5 mole percent and less $BaSnO_3$ a trend of permittivity and grain size is identical to the pure system. For films containing 10 mole percent tin and greater, however, the trend deviates and there is a much greater permittivity reduction.

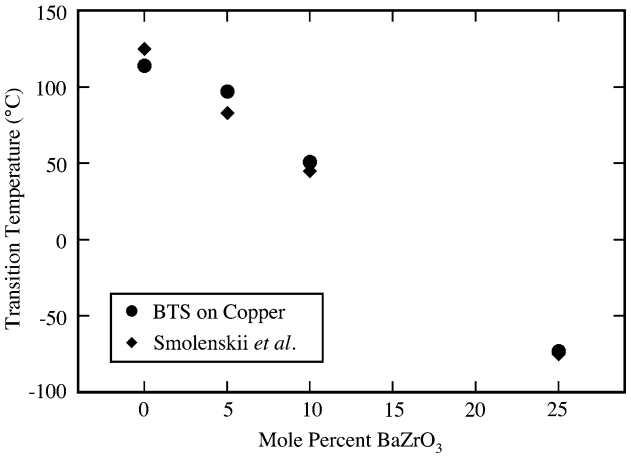

Fig. 7 Phase transition temperature as a function of $BaSnO_3$ level for films on copper and bulk ceramics [9]

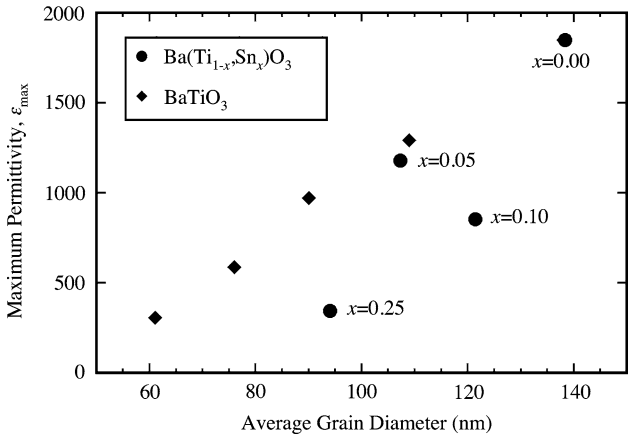

Fig. 8 Permittivity at the phase transition as a function of average grain size for $BaTi_{1-x}Sn_xO_3$ and pure barium titanate [21]

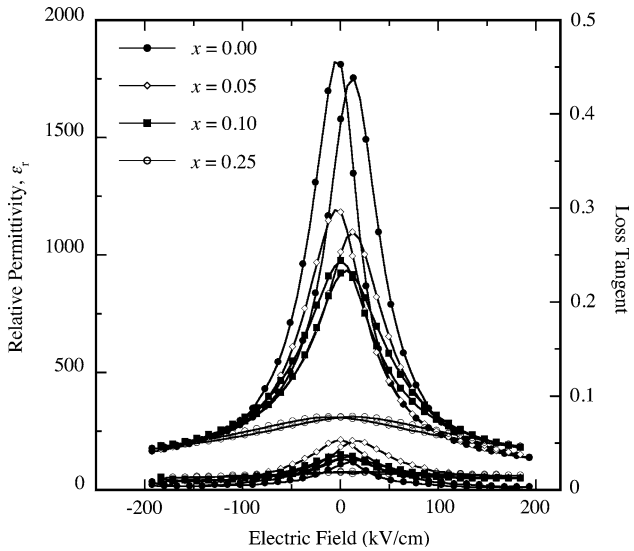

Fig. 9 Field dependence of permittivity and loss tangent for $BaTi_{1-x}Sn_xO_3$ ($0.0 \leq x \leq 0.25$)

The permittivity and loss tangent field dependence was measured at room temperature as shown in Fig. 9. A similar trend of decreasing low-field permittivity with increasing tin level is identified. It is important to note that the high-field permittivity saturates to the same value for each composition. This indicates that the intrinsic lattice response is identical and that the extrinsic ferroelectric response is dampened by the tin addition resulting in diminished dielectric tunability. Though many factors can reduce the nonlinear dielectric response, there are two in the current system that are believed to predominate. The first is a scaling effect associated with an average grain size decrease. The second is an increase in the number and/or strength of domain wall pinning sites. The $Ba(Ti,Zr)O_3$ [24] and $Ba(Ti,Hf)O_3$ [25] systems showed an identical trend of decreasing permittivity with grain size as the pure $BaTiO_3$ system and the $Ba(Ti,Sn)O_3$ system does not, suggesting that the second contributor is dominant in films containing greater than 5% tin. One proposed mechanism is the presence of Sn^{2+} on the normally 4^+ valent B site, which could allow for ionic compensation by oxygen vacancies as shown in Kröger–Vink notation [35] in Eq. (1). This is a reasonable assumption given the low-saturating loss tangents at high fields for each composition.

$$BaO + SnO \xrightarrow{BaTiO_3} Ba_{Ba}^{x} + Sn''_{Ti} + 2O_{O}^{x} + V_{O}^{\bullet\bullet} \quad (1)$$

It is hypothesized that for compositions containing 5% tin and less that the reoxidation anneal was successful in filling oxygen vacancies and changing Sn^{2+} to Sn^{4+} and thus has allowed for the expected grain size and permittivity trend. Kinetic limitations in samples containing 10 and 25% tin likely resulted in materials with a high concentration of Sn^{2+}–$V_O^{\bullet\bullet}$ defect complexes. These defect complexes could then pin domain wall motion and limit the extrinsic ferroelectric contributions to permittivity. This ability of defect dipoles to pin domains and cause aging effects in ferroelectric perovskites is well known [36].

Both $Ba(Ti,Zr)O_3$ and $Ba(Ti,Hf)O_3$ showed the onset of relaxor behavior as the substituent concentration increased [24, 25]. Figure 10 shows the compositional and temperature dependence of permittivity and loss tangent at 1, 10, and 100 kHz. As the tin level increases, there is an increase in the phase transition diffuseness. While relaxor behavior is typically observed at the 20 mole percent level in $Ba(Ti,Sn)O_3$ ceramics, [10, 11] no phase transition temperature frequency dispersion is observed in the thin films, even at the 25 mole percent level. There are two possible explanations for the observed behavior. First, the 25% level is close to the minimum concentration necessary to observe dispersion in the bulk, and it is possible that a higher level is necessary, especially in systems with such fine grains. Second, the likelyhood of Sn^{2+} remaining in the lattice may alter the onset and stability of polar-microregions.

Chemical solution deposited BTS thin films were prepared with compositions containing ranging from 0 to 25 mole percent tin. A processing atmosphere was chosen such that the Sn^{2+} state of tin was stabilized and resulted in a minimization of grain size reduction in comparison with BTZ and barium titanate hafnate. X-ray diffraction patterns reveal single-phase films suggesting tin was fully incorporated into the lattice. A decrease in phase transition temperature and maximum permittivity was observed as the tin level increased. The decrease in permittivity was attributed to a combination of a grain size effect in addition to incomplete stabilization of Sn^{4+}, which resulted in defect-dipole formation and limited extrinsic ferroelectric contributions to the dielectric constant. Frequency-dependent measurements did not reveal phase transition

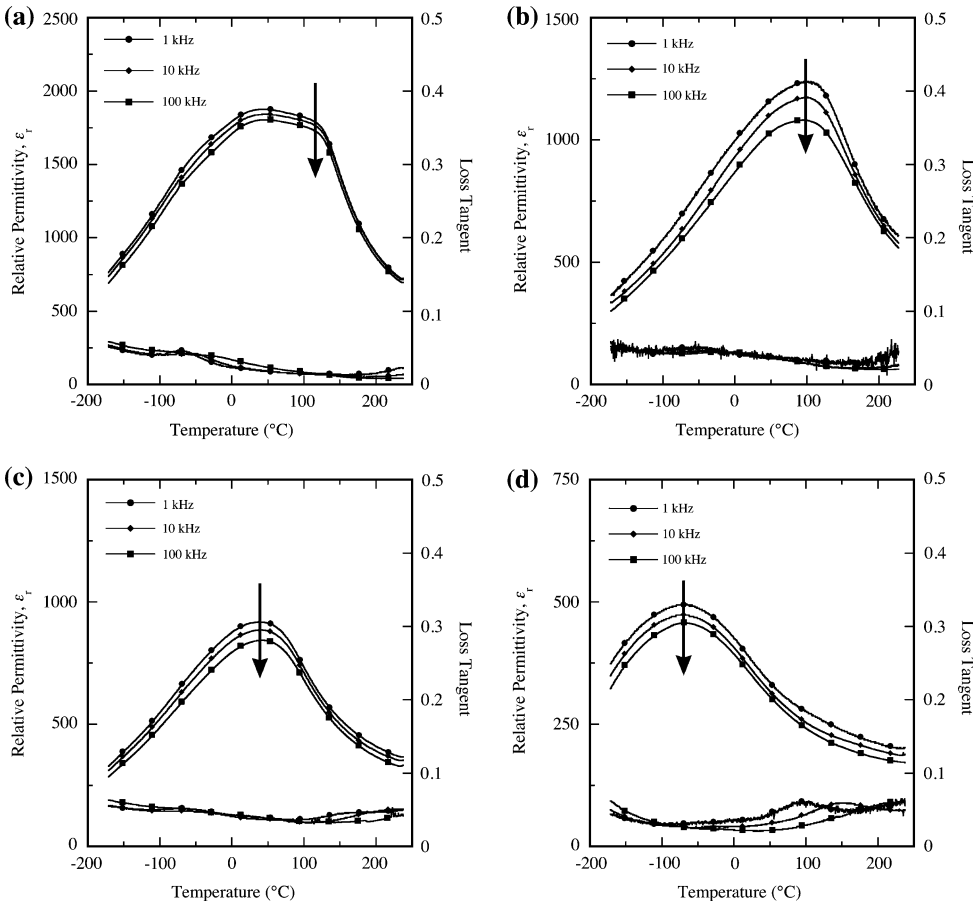

Fig. 10 Temperature and frequency dependence of permittivity and loss tangent for (**a**) $BaTiO_3$, (**b**) $BaTi_{0.95}Sn_{0.05}O_3$, (**c**) $BaTi_{0.90}Sn_{0.10}O_3$, and (**d**) $BaTi_{0.75}Sn_{0.25}O_3$ films

frequency dispersion. It is hypothesized that the 2-valent state of tin may sufficiently alter the dielectric response such that relaxor behavior is not observed.

Acknowledgement The authors wish to acknowledge the financial support of E.I. Du Pont de Nemours and Company.

References

1. Tombak A, Maria JP, Ayguavives F, Jin Z, Stauf GT, Kingon AI, Mortazawi A (2002) IEEE Microw Wirel Co 12:3. doi:10.1109/7260.975716
2. Pervez NK, Hansen PJ, York RA (2004) Appl Phys Lett 85:4451. doi:10.1063/1.1818724
3. Ghosh D, Laughlin B, Nath J, Kingon AI, Steer MB, Maria JP (2006) Thin Solid Films 496:669. doi:10.1016/j.tsf.2005.09.025
4. Kingon AI, Maria JP, Streiffer SK (2000) Nature 406:1032. doi:10.1038/35023243
5. Hofer C, Hoffmann M, Boettger U, Waser R (2002) Ferroelectrics 270:179. doi:10.1080/00150190211242
6. Ihlefeld J, Laughlin B, Hunt-Lowery A, Borland W, Kingon A, Maria J-P (2005) J Electroceram 14:95. doi:10.1007/s10832-005-0866-6
7. Jonker GH (1955) Philips Tech Rev 17:129
8. Novosiltsev NS, Khodakov AL (1956) Sov Phys Tech Phys 1:306
9. Smolenskii GA, Isupov VA (1954) Zh Tekh Fiz 24:1375
10. Mueller V, Beige H, Abicht HP (2004) Appl Phys Lett 84:1341. doi:10.1063/1.1649820
11. Yasuda N, Ohwa H, Asano S (1996) Jpn J Appl Phys, Part 1 35:5099. doi:10.1143/JJAP.35.5099
12. Smolensky GA (1970) J Phys Soc Jpn 28(Suppl):26
13. Mueller V, Beige H, Abicht HP, Eisenschmidt C (2004) J Mater Res 19:2834. doi:10.1557/JMR.2004.0386
14. Kuo YF, Tseng TY (1999) Electrochem Solid-State Lett 2:236. doi:10.1149/1.1390795
15. Yoon KH, Park JH, Jang JH (1999) J Mater Res 14:2933. doi:10.1557/JMR.1999.0392
16. Zhai JW, Shen B, Yao X, Zhang LY (2004) J Am Ceram Soc 87:2223. doi:10.1111/j.1151-2916.2004.tb07495.x
17. Zhai J, Shen B, Yao X, Zhang L (2004) Mater Res Bull 39:1599. doi:10.1016/j.materresbull.2004.05.010
18. Halder S, Victor P, Laha A, Bhattacharya S, Krupanidhi SB, Agarwal G, Singh AK (2002) Solid State Commun 121:329. doi:10.1016/S0038-1098(02)00017-0
19. Nakagauchi R, Kozuka H (2007) J Sol-Gel Sci Technol 42:221. doi:10.1007/s10971-007-0772-2
20. Song S, Zhai JW, Yao X (2007) J Sol-Gel Sci Technol 44:75. doi:10.1007/s10971-007-1604-0
21. Ihlefeld JF, Vodnick AM, Baker SP, Borland WJ, Maria J-P (2008) J Appl Phys 103(7):074112
22. Dawley JT, Clem PG (2002) Appl Phys Lett 81:3028. doi:10.1063/1.1516630
23. Dawley JT, Ong RJ, Clem PG (2002) J Mater Res 17:1678. doi:10.1557/JMR.2002.0247
24. Ihlefeld JF, Borland W, Maria J-P (2005) J Mater Res 20:2838. doi:10.1557/JMR.2005.0342

25. Ihlefeld JF, Borland WJ, Maria J-P (2008) Thin Solid Films 516:3126. doi:10.1016/j.tsf.2007.08.096
26. Ihlefeld JF, Borland WJ, Maria J-P (2008) Scr Mater 58:549. doi:10.1016/j.scriptamat.2007.11.008
27. Ihlefeld JF, Borland WJ, Maria J-P (2007) Adv Funct Mater 17:1199. doi:10.1002/adfm.200601159
28. Hoffmann S, Waser R (1999) J Eur Ceram Soc 19:1339. doi:10.1016/S0955-2219(98)00430-0
29. Schwartz RW, Clem PG, Voigt JA, Byhoff ER, Van Stry M, Headley TJ, Missert NA (1999) J Am Ceram Soc 82:2359
30. Barin I (1995) In: Thermochemical data of pure substances VCH. Weinheim, New York
31. Yang GY, Dickey EC, Randall CA, Barber DE, Pinceloup P, Henderson MA, Hill RA, Beeson JJ, Skamser DJ (2004) J Appl Phys 96:7492. doi:10.1063/1.1809267
32. Ihlefeld JF, Losego MD, Collazo R, Borland WJ, Maria JP (2008) J Mater Sci 43:38. doi:10.1007/s10853-007-2135-3
33. Nelson JB, Riley DP (1945) Proc Phys Soc Lond 57:160. doi:10.1088/0959-5309/57/3/302
34. ASTM E 112-96 (2003) In: Standard test methods for determining average grain size. ASTM International, West Conshohocken, PA
35. Kröger FA, Vink HJ (1956) Solid State Phys 3:307
36. Jaffe B, Cook WR, Jaffe HLC (1971) In: Piezoelectric ceramics. Academic Press, London, New York